Journal of Earth Science, *2017 online* *ISSN 1674-487X*
Printed in China
DOI: 10.1007/s12583-017-0938-y

Radiolarian and detrital zircon in the Upper Carboniferous to Permian Bancheng Formation, Qinfang Basin, and the geological significance

Xue Ke[1], Zongyan Zhang[2], Jianghai Yang[3, 4], Huazhou Yao[2], Shengdong Wang[1], Weihong He[3, 4*]
1. *Institute of Geological Survey*, *China University of Geosciences*, *Wuhan 430074*, *China.*
2. *Wuhan Center of China Geological survey*, *Wuhan 430205*, China.
3. *State Key Laboratory of Biogeology and Environmental Geology*, *China University of Geosciences*, *Wuhan 430074*, PR China.
4. *Faulty of Earth Sciences*, *China University of Geosciences*, *Wuhan 430074*, China.

ABSTRACT: The Bancheng Formation exposed along the Shiti Reservoir nearby Bancheng Town, Qinfang Basin, southern Guangxi, is mainly composed of thin-bedded chert. The radiolarian assemblages in the studied section suggest it was a pelagic setting and the age of the Bancheng Formation is Late Carboniferous to Early Permian. The detrital zircon U-Pb ages from the section are characterized by a Permian peak at ~282 Ma. Detrital zircon provenance analysis suggests that the Permian detrital zircons in the Bancheng Formation were likely from volcanic-magmatic arc rocks related to the subduction of the Paleo-Tethyan Ocean. The long-lived deposition (from Upper Devonian to Middle Permian, about 125 Myrs) of the radiolarian cherts in the Qinfang Basin was comparable with that deposited in Ailaoshan Ocean. The radiolarian assemblages in Qinfang Basin show a Tethyan affinity. Together with the Permian subduction-related arc volcanic rocks and the E-MORB type basalts to the northwest of the study area, our data support the existence of a Permian arc-related basin in the Qinfang area.
KEY WORDS:Qinfang Basin, Bancheng Formation, detrital zircon, Radiolarian, Permian arc-related basin.

0 INTRODUCTION

The Qinfang area in southern Guangxi was part of the Paleo-Tethys tectonic domain in the late Paleozoic (Zhao et al., 2007). A Paleozoic deep-sea depositional succession outcrops in the area (Wang, 1994; Ma, 1996). According to studies on the fossils and geochemistry of the upper Paleozoic cherts in the area (Wang, 1994; Zhang et al., 2002, 2008; Sun and Xia, 2006; Hu, 2014), some researchers have suggested that it was an intracontinental rift (Liu et al., 1993a), an expanded residual trough (Zhang et al., 1998; Xu et al., 2001), or a passive continental margin during the late Paleozoic (Yu et al., 1989; Deng et al., 2003; Zhao et al., 2007). Additionally, others have argued that it was a part of the Paleo-Tethys Ocean (Wu et al., 1994a; Wu, 1999, 2003) or an ocean basin during the late Paleozoic according to several lines of evidences, including the subduction-related arc volcanic rocks (lower Indosinian granites), the presence of pelagic radiolarian assemblage and absence of benthic fauna (Qin et al., 2011, 2012, 2013; He et al., 2014; Zhang et al., 2016).

*Corresponding author: whzhang@cug.edu.cn.

Manuscript received January16, 2017.
Manuscript accepted July 12, 2017.

In this paper, radiolarian assemblages are reported from the Upper Carboniferous to Permian Bancheng Formation in the Qinfang area and indicate a deep sea or pelagic setting. Furthermore, we studied the provenance of the Bancheng Formation i using detrital zircon U-Pb ages. These data then used to discuss the tectonic setting of the Qinfang Basin during the late Paleozoic.

1 GEOLOGICAL SETTING

The South China Block comprises the Yangtze and Cathaysia blocks, both of which were divided by an orogenic belt from Qinzhou Bay to Hangzhou Bay (Yang and Mei, 1997; Fig. 1). The Qinfang Basin is a Early Silurian to Middle Permian, elongated sedimentary basin in the southwest of the Qingzhou-Hangzhou Metallogenic Belt (Xu et al., 2012). The Qinfang Basin is adjacent to the Yunkai Massif to the southeast, adjacent to the Shiwandashan Basin to the northwest, and adjacent to the Northeast Vietnam terrane to the southwest (Fig. 1).

The Shiwandashan Basin contains upper Paleozoic to Mesozoic successions (Liang et al., 2004; Liang and Li, 2005). Lower Mesozoic acidic volcanic rocks are exposed on both sides of the Shiwandashan Basin (Qin et al., 2011). The Middle

Triassic unconformity covered the Lower Triassic succession and corresponds to the widespread intrusion of Indosinian-aged granites into the pre-Middle Triassic strata (BGMRGR, 1985; Deng et al., 2004; Zhao et al., 2010; Qin et al., 2013). The Yunkai Massif represents a basement block adjacent to the Qinfang Basin. The massif comprises mainly Precambrian metamorphic complexes, Neoproterozoic metasedimentary and metaigneous rocks (amphibolite-facies), and upper Neoproterozoic to lower Paleozoic clastic rocks (BGMRGR, 1985; BGMRGP, 1988; Huang et al., 2001; Qin et al., 2006; Yu et al., 2010; Zhang et al., 2012a).The Northeast Vietnam terrane which separated from the northwest and central Vietnam by Red River Fault consists of a Paleozoic-lower Mesozoic succession of magmatic and metamorphic rocks covering a Precambrian metamorphic basement (Lepvrier et al, 1997; Roger et al., 2000, 2012; Yan et al., 2006; Hoa, et al., 2008; Chen et al., 2014; Faure et al., 2014). The ophiolitic mélange discovered in Babu and in the Song Hien belt marks the northern margin of the terrane and is interpreted as the trace of an oceanic suture between the Indochina and South China blocks (Wu et al., 1999; Cai and Zhang, 2009; Halpin et al., 2016; Yang et al., 2017). The Jinshanjiang-Ailaoshan belt which represents the main and branch oceans respectively (Liu et al. 1993b; Zhong 1998; Wang et al., 2000; Jian et al., 2009b) extends southward into Vietnamman along the Song Ma suture (Metcalfe, 2011).

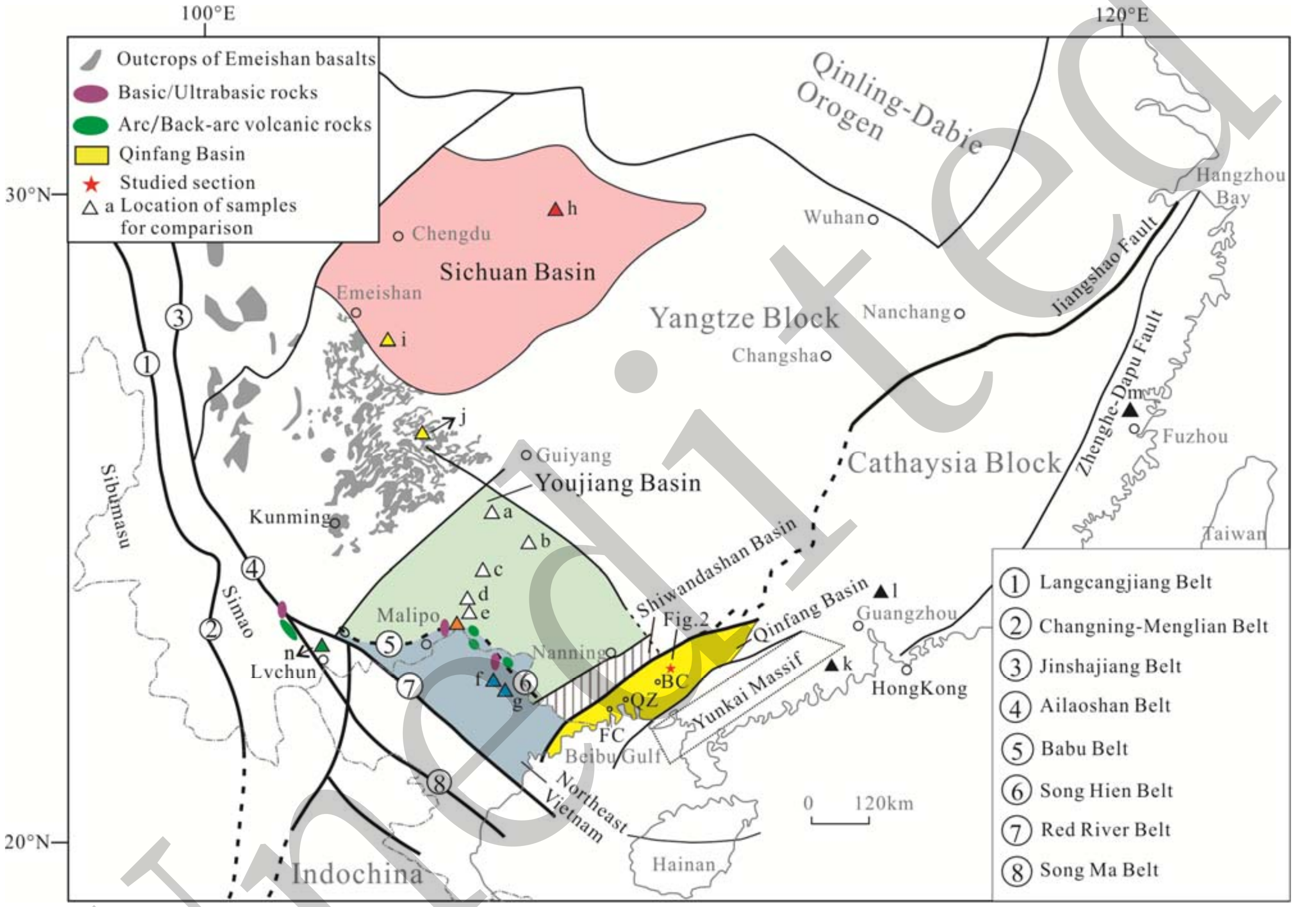

Figure 1. Tectonic map of South China and adjacent areas (according to Sone et al., 2008, 2012; Yang et al., 2012; Hu et al., 2015). The distribution of the Emeishan volcanic province is revised from He et al. (2007); Yang et al., (2015). The distribution of the basic/ultrabasic rocks and arc/back-arc volcanic rocks is revised from Zhong et al. (1998), Wu et al., (2002), Halpin et al., (2016), Jian et al . (2009a, 2009b), Fan et al., (2010), Liu et al. (2011), Li., (2013), Lai et al., (2014).The locations of the samples for comparison with the Bancheng Formation in detrital zircon ages are marked as triangles with different colors ((i-j) He et al., 2007; (a-e) Yang et al., 2012, 2013, 2015, 2017; (n) Li et al., 2013; (h-m) Liang et al., 2013; (f-g) Halpin et al., 2016). Abbreviations: FC, Fangcheng; QZ, Qinzhou; BC, Bancheng;

The northeast-trending Bancheng Formation outcrops in the southeastern area of Bancheng and Xiaodong. The lower part of the Bancheng Formation is composed of pale grayish-yellow radiolarian chert and siliceous mudstone intercalated with small amounts of grayish-red chert. The middle and upper parts are composed of grayish-red radiolarian chert and siliceous mudstone intercalated with grayish-yellow chert and mudstone. The radiolarians obtained from the Bancheng Formation reveal that the Bancheng Formation was deposited in the Late Carboniferous to Permian (GXBGMR, 1985; Wu et al., 1994b; Wang et al. 1994, 1998).

The Shiti section studied in this paper is located on the northern side of the Shiti Reservoir, 4 km from Bancheng Town, Qinzhou City, Guangxi Zhuang Autonomous Region (Fig. 1). The strata of the Bancheng Formation at the studied section are heavily deformed and comprise 14 east-directed rock slices divided by a series of the high-angle, imbricated, thrust faults in the section. Each slice is composed of thin-bedded chert intercalated with siliceous siltstone, tuff and manganese sandstone (Figs. 2 and 3). Radiolarian and zircon samples were collected systematically from the studied section of the Bancheng Formation (Fig. 3).

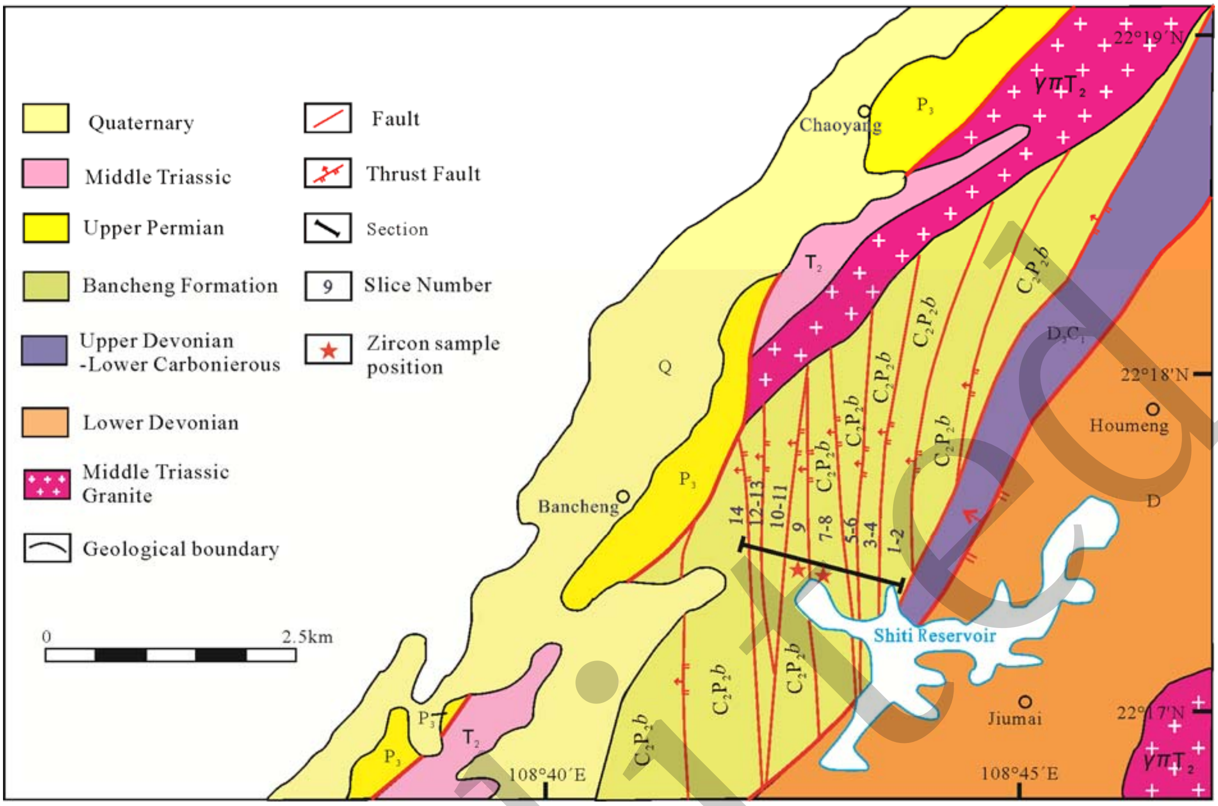

Figure 2. Geological map of the study area (modified from Geological Survey of Guangxi, 2010).

2 SAMPLES AND METHODS

2.1 Radiolarian sampling and analyses

We systematically collected chert samples for radiolarian analysis from each slices of the Bancheng Formation in the studied section. All samples were etched in a 1-5% solution of HF for 4-8 hrs at room temperature. The acid residues were subsequently transferred to other containers filled with water until neutral. Residual samples were immersed in new HF solution. After repeating this process more than 40 times, adequate residues were sieved with a mesh diameter of 0.054 mm and dried for examination. We examined each species primarily under a binocular microscope, then selected some specimens from each species for scanning electron microscopy, and finally re-examined each species for morphological consistency (He et al., 2011). We obtained radiolarians from slices 1, 4, 6, 7, 9, and 12 (Fig. 3).

2.2 Detrital zircons sampling and dating

Two samples (samples ST-7W and ST-9W) were collected for detrital zircon dating. Sample ST-7W is a tuffaceous and siliceous sandstone collected from slice 7 in the studied section. Sample ST-9W is a tuffaceous and sandy chert collected from slice 9 of the studied section. The sample positions are shown in Fig. 2.

The detrital zircons were first separated from the crushed rocks using conventional heavy liquid and magnetic techniques then individually picked under a binocular microscope. The zircons from each sample were randomly selected, enclosed in epoxy resin and polished to approximately half their thickness. The zircons were then photographed under reflected and transmitted light. Cathodoluminescence (CL) imaging of zircons was performed using a JSM-IT100 scanning electron microprobe equipped with a Gatan cathodoluminescence system at Wuhan Sample Solution Analytical Technology Co. Ltd.

The U-Pb dating of zircons was conducted using LA-ICP-MS at the State Key Laboratory of Geological Processes and Mineral Resources, China University of Geosciences, Wuhan. Detailed operating conditions for the laser ablation system and ICP-MS instrument and the data reduction techniques are the same as those described by Liu et al. (2008; 2010a; 2010b). Laser sampling was performed using a GeoLas 2005. An Agilent 7500a ICP-MS instrument was used to acquire ion-signal intensities. A “wire” signal smoothing device included in this laser ablation system enabled smooth signals to be produced even at laser repetition rates as low as 1 Hz (Hu et al., 2012). Helium was used as the carrier gas. Argon was used as the make-up gas and was mixed with the carrier gas via a T-connector before the mixture entered the ICP. Nitrogen was added to the central gas flow (Ar+He) of the Ar plasma to decrease the detection limit and improve precision (Hu et al., 2008; Liu et al., 2010b). Each analysis incorporated a background acquisition of approximately 20-30 s (gas blank) followed by 50 s of data acquisition from the sample. An

Agilent Chemstation was utilized to perform each individual analysis. The selection and integration of the background and analyte signals and the temporal drift corrections were performed off-line. Zircon 91500 was used as the external standard for U-Pb dating and was analyzed twice every 5 analyses. Time-dependent drifts in the U-Th-Pb isotopic ratios were corrected using a linear interpolation over time every five analyses, according to the variations in 91500 (i.e., 2 zircon 91500 + 5 samples + 2 zircon 91500) (Liu et al., 2010a). The preferred U-Th-Pb isotopic ratios used for 91500 are from Wiedenbeck et al. (1995). The uncertainty in the preferred values for the external standard 91500 was propagated to the final results for the samples. Concordia diagrams and weighted mean calculations were made using Isoplot/Ex_ver3 (Ludwig, 2003). Concordance = 100 * (1 - abs($^{206}Pb/^{238}U$ Age - ^{207}Pb / ^{235}U Age) / (($^{206}Pb/^{238}U$ + ^{207}Pb / ^{235}U) / 2)))

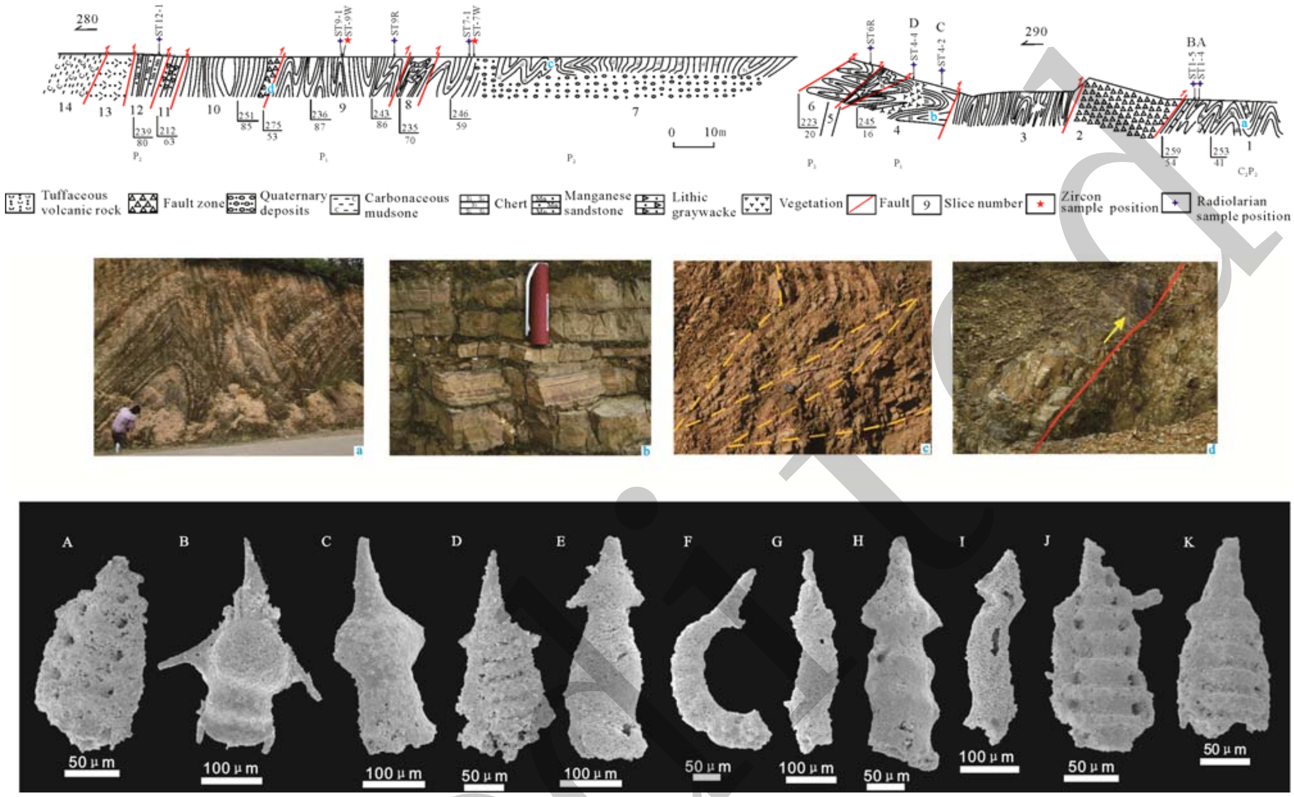

Figure 3. (a) Cross-section of the Bancheng Formation, Shiti Reservoir, Bancheng Town, Qinzhou City, Guangxi. (b) Field photos of the cross-section, (1): recumbent homoclinal fold in slice 1; (2): Bouma sequence in slice 4; (3): inclined tight fold in slice 7; (4): thrust fault between slice 9 and slice 10. (c) SEM photos of the radiolarians from the cross-section, **A, D, J, K** *Albaillella xiaodongensis*: **A** 13ST1-4-082, Slice 1; **D** 13ST4-4-168, Slice 4; **J** 13ST12-1-132, Slice 12; **K** 13ST12-1-135, Slice 12; Age: P_1; **B** *Pseudoalbaillella globosa*: 12ST1-5R-082k, Slice 1, Age: P_2; **C** *Pseudoalbaillella rhombothoracata*: 12ST4-2R-082, Slice 4, Age: P_2; **E** *Pseudoalbaillella internata*: 12ST6R-145, Slice 6, Age: P_2; **F** *Pseudoalbaillella u-forma*: 13ST7-1-046, Slice 7, Age: P_1; **G** *Pseudoalbaillella elegans*: 13ST7-1-047, Slice 7, Age: P_1; **H P***seudoalbaillella nodosa*: 12ST9R-182, Slice 9, Age: C_2; **I** *Pseudoalbaillella elegans*: 13ST9-1-083, Slice 9, Age: P_1.

3 RESULTS

3.1 Radiolarians

The strata of slice 1 yield the radiolarian fossils: *Albaillella xiaodongensis*, *Pseudoalbaillella longicornis*, *Latentifistula texana*, *Pseudoalbaillella globosa*, *Pseudoalbaillella fusiformis*, *Pseudoalbaillella yanaharensis*, *Pseudoalbaillella longicornis*, *Latentifistula texana*, *Entactinia itsukaichiensis*, *Pseudoalbaillella lomentaria*, and *Pseudoalbaillella sakmarensis*.

The strata of slice 4 contain the following radiolarian fossils: *Pseudoalbaillella rhombothoracata*, *Albaillella xiaodongensis*, *Latentifistula texana*, *Latentifistula crux*, and *Latentifistula asperspongiosa*.

The strata of slice 6 yield the radiolarian fossils: *Pseudoalbaillella globosa*, *Latentifistula banchengensis*, *Pseudoalbaillella internata*, *Ruzhencevispongus uralicus*, *Latentibifistula asperspongiosa*, and *Quinqueremis robusta*.

The strata of slice 7 yield the radiolarian fossils: *Pseudoalbaillella u-forma*, *Pseudoalbaillella elegans*, *Pseudoalbaillella reflexa*, and *Pseudoalbaillella rhombothoracata.*

The strata of slice 9 yield the radiolarian fossils: *Pseudoalbaillella nodosa*, *Pseudoalbaillella bulbosa*, *Pseudoalbaillella elegans*, *Latentifistula mushroomformis*, *Pseudoalbaillella u-forma*, *Pseudoalbaillella elegans*, and *Pseudoalbaillella reflexa*.

The strata of slice 12 yield radiolarian *Albaillella xiaodongensis*.

3.2 Detrital zircon U-Pb ages

The zircons from the two samples are generally transparent to semi-transparent, euhedral, subhedral or rounded crystals that are 50-150 μm in size and have width/length ratios of 1:1-1:3. Most grains show oscillatory zoning in CL images (Fig. 4). A total of 156 zircons from the two samples were dated. Of these, 139 spots yielded concordant ages, and 137 of the zircons have Th/U ratios > 0.1, the other 2 zircons have Th/U ratios<0.1 (Fig. 5), indicating a probable magmatic origin for the majority of the analyzed zircons (Belousova et al., 2002).

Of the 110 analyses on 110 zircons from sample ST-7W, 106 are concordant (concordance≥95%; Fig. 6a). The measured ages range from 2813 Ma to 265 Ma. One major age group occurs at 300-265 Ma (34 grains), with the main peak age at 274 Ma Subordinate age groups are observed at 394-301 Ma (11 grains), 641-495 Ma (6 grains), 894-726 Ma (12 grains), 1165-904 Ma (23 grains), 1827-1254 Ma (10 grains), and 2813-2150 Ma (9 grains) (Table 1, Fig. 6c).

Of the 46 analyses on 46 zircons from sample ST-9W, 33 are concordant (concordance≥95%; Fig. 6b). The measured ages range from 1835 Ma to 265 Ma. One major age group occurs at 304-277 Ma (19 grains), with the main peak age at 294 Ma. Subordinate age groups are observed at 1000-904 Ma (5 grains), 643-413 Ma (7 grains), and 1835-1813 Ma (2 grains) (Table 2, Fig. 6d). Only one scattered zircon yielded the age of 265 Ma.

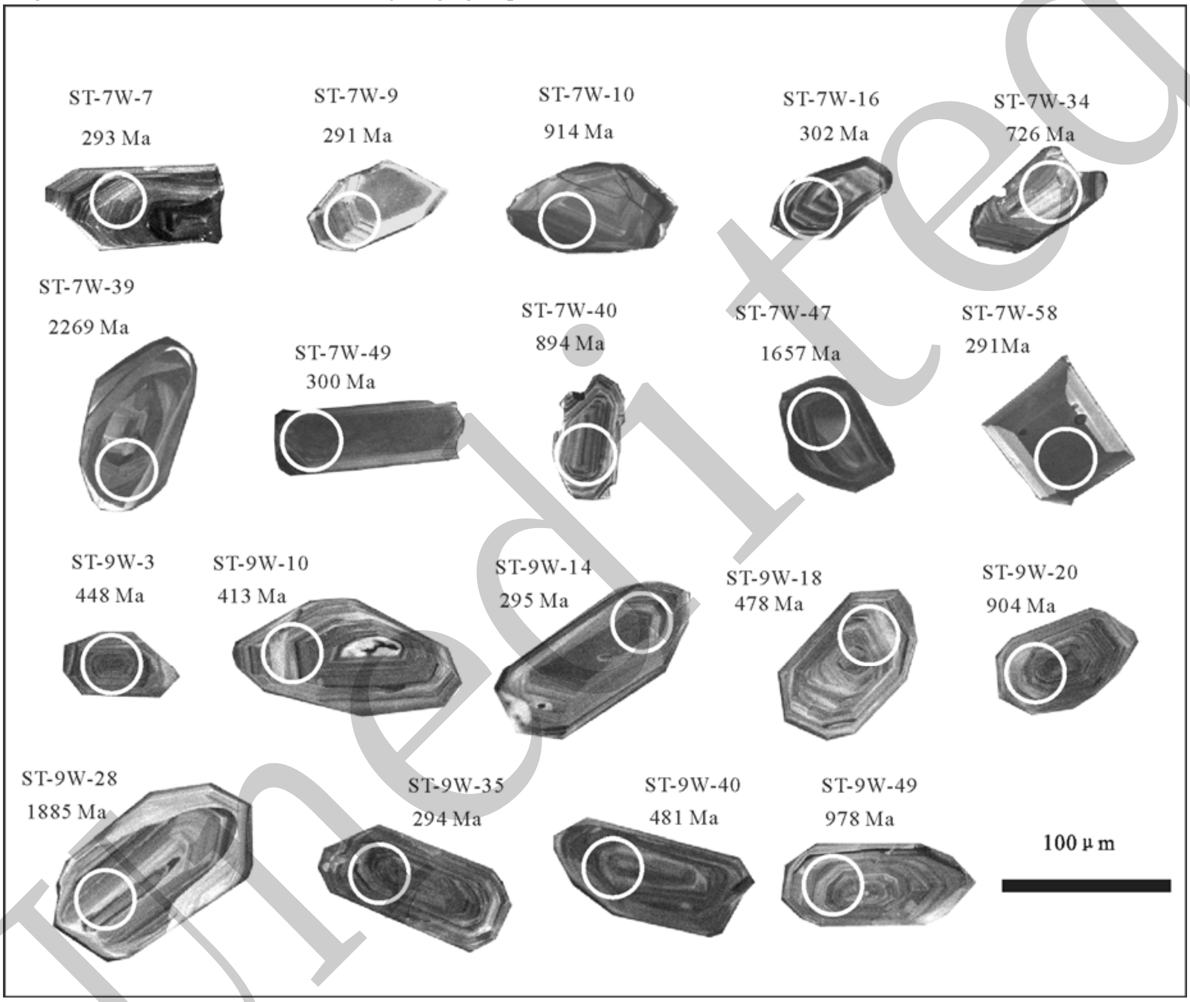

Figure 4. Cathodoluminescence (CL) images of representative detrital zircons analyzed for U-Pb ages from samples ST-7W and ST-9W from the Bancheng Formation, Qinfang Basin. Circles indicate the in situ analytical spots measured to obtain the U-Pb ages.

4 DISCUSSION

4.1 The age of the Bancheng Formation

In slice 1 of the studied section, four Late Carboniferous to Middle Permian radiolarian assemblages were identified: the Middle Permian *Albaillella xiaodongensis* and *Pseudoalbaillella globosa* assemblages, the Early Permian P*seudoalbaillella lomentaria-Pseudoalbaillella sakmarensis* assemblage, and the Late Carboniferous *Pseudoalbaillella nodosa* assemblage**.** Therefore, the age of slice 1 is likely Late Carboniferous to Middle Permian.

In slice 4 of the studied section, two Early Permian radiolarian assemblages were identified: th *Pseudoalbaillella rhombothoracata* and A*lbaillella xiaodongensis* assemblages. Therefore, slice 4 is mainly composed of sediments formed during Early Permian.

In slice 6 of the studied, tfossils *Pseudoalbaillella globasa* and *Pseudoalbaillella monacanthus* were identified. Additionally, abundant *Latentifistula banchengensis*,

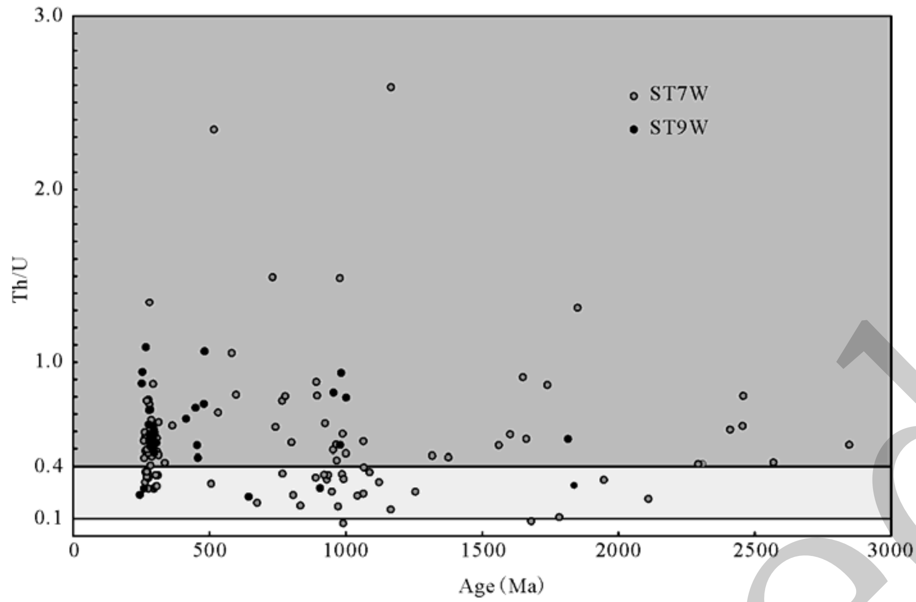

Figure 5. Ages (Ma) versus Th/U ratios for samples ST-7W and ST-9W from the Bancheng Formation, Qinfang Basin.

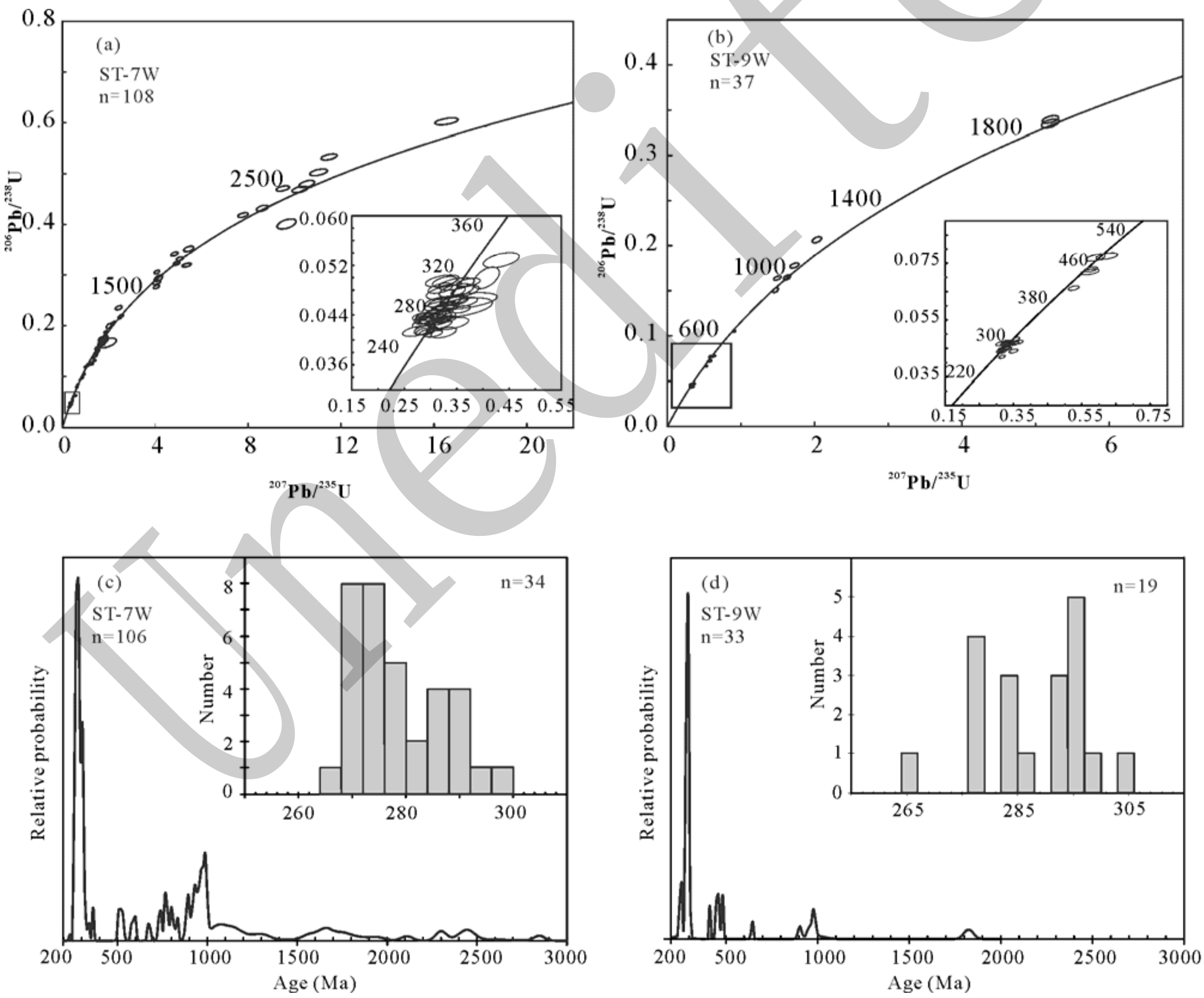

Figure 6. Concordia diagrams ((a) and (b)) and probability density diagrams ((c) and (d)) of zircon U-Pb data for samples ST-7W and ST-9W from the Bancheng Formation, Qinfang Basin. The numbers represent the number of zircons measured.

Pseudoalbaillella internata, *Ruzhencevispongus uralicus*, and *Latentibifistula asperspongiosa* were observed, and a small number of *Quinqueremis robusta* were also identified in this slice. Therefore, the age of slice 6 is likely Middle Permian.

In slice 7 of the studied section, two Early Permian radiolarian assemblages were identified: the *Pseudoalbaillella u-forma-Pseudoalbaillella elegans* assemblage and the *Pseudoalbaillella rhombothoracata* assemblage. These radiolarian fossils are consistent with youngest detrital zircon group with ~274 Ma age peak, suggesting that the age of slice 7 is likely Middle Permian

In slice 9 of the studied section, three Late Carboniferous to Early Permian radiolarian assemblages were identified: the *Pseudoalbaillella nodosa* assemblage, the *Pseudoalbaillella bulbosa* assemblage, and the *Pseudoalbaillella u-forma-Pseudoalbaillella elegans* assemblage. Combined with the youngest detrital zircon age group with ~294 Ma age group, the age of slice 9 is probably of Early Permian.

In slice 12 of the studied section, one Middle Permian radiolarian assemblage was identified: the *Albaillella xiaodongensis* assemblage. Therefore, slice 12 is mainly composed of Middle Permian strata.

The radiolarian assemblages and the youngest detrital zircon age groups indicate that the age of the studied section is likely Late Carboniferous to Middle Permian, and the age of slice 7 and slice 9 is Early to Middle Permian.

4.2. Detrital zircon provenance

Detrital zircon dating has been widely applied to identify the provenances of sediments and to characterize tectonic events (Condie et al., 2009; Yang et al., 2012, 2014; Cawood et al. 2012; Li et al., 2012). The detrital zircon U-Pb ages from the Bancheng Formation range from Archean to late Paleozoic, with prominent age groups of 1165-904 Ma, 528-413 Ma, and 300-265 Ma and subordinate age groups of 2813-2403 Ma, 1835-1548 Ma, and 894-580 Ma (Fig. 8e). The age group 1165-904 Ma, with a peak age of 991 Ma (Fig. 8e), is inferred to have been derived from the Neoproterozoic metabasite exposed along the northern the Yunkai Massif to the southeast of the Qinfang area (Fig. 7a; Zhang et al., 2012a).The age group 528-413 Ma, with a peak age of 455 Ma (Fig. 8e), is likely derived from the lower Paleozoic granites and granulites in the Wuyi-Yunkai orogen (Fig. 7a; Peng et al., 2006; Wang et al., 2007, 2011, 2013; Li et al., 2010; Yang et al., 2010). The age groups of 2813-2403 Ma, 1835-1548 Ma, and 894-580 Ma are inferred to be respectively derived from the reworked basement units (Hu., 2015), including the Paleoproterozoic-Mesoproterozoic granites exposed on the Yunkai area or on Hainan Island (Fig. 7a, 7b; Peng, 2000; Li et al., 2002, 2008; Qin et al., 2006), and multi-cycle sedimentary sources in the Yunkai Massif or reworked Paleozoic units in the Qinfang area (Hu et al., 2015). The 300-265 Ma age group were most likely derived from Jinshajiang-Ailaoshan belt ((Fig. 7c; Jian et al., 1999, 2008; Wang et al., 2011; Yan et al., 2006; Hening et al., 2009; Fan et al., 2010; Li, 2013; Lai et al., 2014). An alternative source could be Hainan Island (Fig. 7b; Li et al., 2002, 2006, 2008, Xie et al. ,2005, 2006,Chen et al., 2011, Tang et al., 2013), either Southeast Yunnan-North Vietnam (Fig. 7d; Roger et al, 2000, Hoa et al, 2008; Zhang et al., 2013; Chen et al., 2014; Halpin et al., 2016).

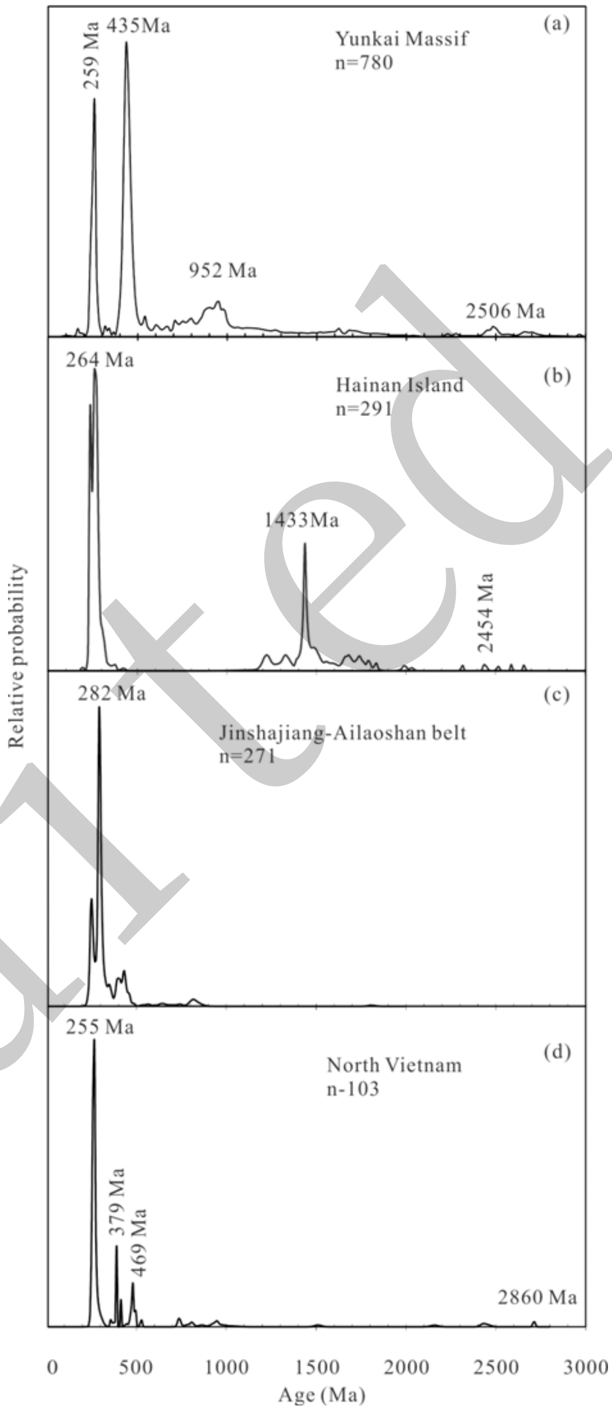

Figure 7. Probability density diagrams of zircon U－Pb age from different areas within the South China ((a) Yunkai Massif – Yu et al. (2010), Wang et al. (2011), Peng et al. (2006), Qin et al. (2006), Zhang et al. (2012), Chen et al. (2011, 2012), Zhao et al. (2010); (b) Hainan Island – Chen et al. (2011), Li et al. (2002, 2006, 2008), Tang et al. (2013), Xie et al. (2006); (c) Jinshanjiang - Ailaoshan and Song Ma suture zone – Roger et al. (2000), Yan et al. (2006), Peng et al. (2008), Jian et al. (2008), Hoa et al. (2008), Henning et al. (2009), Wang et al. (2011)) (d) Southeast Yunnan-North Vietnam – Roger et al. (2000), Hoa et al. (2008); Zhang et al.. (2013); Halpin et al. (2016)

4.3 Tectonic setting

This paper mainly focused on the 300-265 Ma age group in order to determine the tectonic setting of the studied area in the Permian. As mentioned above, the youngest detrital zircon age group from the Bancheng Formation in the Qinfang area is 300-265 Ma, with the main peak age at ~ 282 Ma (Fig. 8e). In contrast, abundant basaltic and rhyolitic lithic fragments with a single detrital zircon spectrum peak at ~260 Ma presented in the sediments of Upper Permian in the Youjiang Basin (Fig. 8a; Yang et al., 2012b, 2013, 2015), Sichuan Basin and Guizhou in the Yangtze Block (Fig. 8b; He et al., 2007; Liang et al., 2013). These zircons were at ~260 Ma and were derived from the basalts and volcanic rocks of the Emeishan Large Igneous Province (Zhou et al.,2000; He et al., 2007; Yang et al., 2012b, 2013, 2014, 2015; Liang et al., 2013). Significance differences exist between the detrital zircon age spectra of the Qinfang area and those of the Yangtze Block. Furthermore, detrital zircons from the Permian sediments in the western Ailaoshan belt are featured by 300-285 Ma age group (Li, 2013). The zircons in this age group were derived from the magmatic rocks in the western Ailaoshan suture zone (with age of 290-250 Ma) (Jian et al., 2009b; Fan et al., 2010; Li, 2013; Lai et al., 2014) and were associated with the volcanic arc resulted by the westward subduction of the Ailaoshan Ocean (Jian et al., 2009a, 2009b). The youngest detrital zircon age group from the Upper Permian sediments in the Cathaysia Block is 300-260 Ma (Liang et al., 2013), and these zircons were most likely derived from the southwestern Cathaysia Block (Hainan Island) (Li et al., 2006; Xie et al. 2006), suggesting the subduction of the Paleo-Tethyan Ocean (Liang et al., 2004; Liang and Li, 2005). The Early Permian sandstones in the Song Hien tectonic zone and Babu in southeastern Yunnan are featured by a 290-255 Ma zircon age group (Fig. 8c; Halpin et al., 2016) and a 290-280 Ma zircon age group (Fig. 8d; Yang et al., 2017) respectively, both of which were derived from the volcanic rocks exposed in the Babu-Song Hien belt (Hoa et al., 2008; Zhang et al., 2013; Chen et al., 2014; Halpin et al., 2016). These rocks represent the Permian magmatic arc related to the subduction of Babu-Song Hien Paleo-Tethyan Ocean (Wu et al., 2002; Yang et al., 2012a; Halpin et al., 2016). Thus, the Permian sources of the detrital zircons in the Bancheng Formation were similar to the volcanic-magmatic sources related to the subduction of the Paleo-Tethyan Ocean or its branch ocean, suggesting that the Qinfang Basin was adjacent to an active volcanic-magmatic sources related to the subduction of the Paleo-Tethyan Ocean.

The study of radiolarians shows that Albaillellaria (order), which lived in deep marine to bathyal settings with water depths of >500 m (Kozur, 1993), is the dominant element for the Permian radiolarian fauna in the Bancheng Formation in the Qinfang Basin. More importantly, the radiolarian chert successions in the Qinfang Basin deposited from the Upper Devonian to the middle Permian (Wang, 1994), i.e., lasted approximately for 125 Myrs in geological age. By contrast, the Wufeng Formation in South China, representing an interplatform basin, was deposited during the Late Katian to Early Hirnantian in the Late Ordovician (lasted for 3 Myrs) (CCS, 2014). The Gufeng Formation and the Dalong Formation in South China, also representing an interplatform basin, were deposited respectively during the late Roadian-Wordian of the Guadalupian (4 Myrs) and the Changhsingian of the Lopingian (2 Myrs) (CCS, 2014). Additionally, the radiolarian chert in the Ailaoshan Ocean Basin was deposited from the Middle Devonian to the Middle Triassic, i.e., ~160 Myrs (Yang et al., 2010). Thus, the age range of the radiolarian chert in the Qinfang Basin was much longer than that of the chert in the interplatform basin but similar to that of the chert in ocean settings (such as Ailaoshan). Therefore, the evolution of Qinfang Basin and Ailaoshan Ocean was synchronous and correlative. Additionally, other deep-water elements including *Pseudoalbaillella yanaharensis* and *Pseudoalbaillella reflexa* have been found in the Bancheng Formation except for *Pseudoalbaillella elegans*, *Pseudoalbaillella bulbosa* and *Pseudoalbaillella u-forma* (Wang et al., 2012). Thus, the radiolarian assemblages in Qinfang Basin show a Tethyan affinity.

In addition, the lower Mesozoic acidic volcanic rocks exposed along the Pinxiang-Chongzuo area northwest to the Qinfang Basin, are typical for subduction-related arc volcanic rocks (Qin et al., 2011). The Permian E-MORB type basalts that formed in a back-arc setting are distributed along the Pinxiang-Chongzuo area (Qin et al., 2012). All these lines of evidence support that the Qinfang area was an arc-related basin in Permian.

5 CONCLUSION

(1) The radiolarian assemblages and the data of detrital zircon age in the studied section indicate that the age of the Bancheng Formation is Late Carconiferous-Middle Permian.

(2) The Qinfang Basin and Ailaoshan Ocean have a synchronous and correlative evolution. The radiolarian assemblages in Qinfang Basin show a Tethyan affinity.

(3) The sources of the detrital zircons with Early-Permian ages from the Bancheng Formation are likely the volcanic-magmatic arc rocks related to the subduction of the Paleo-Tethyan Ocean. Together with the Permian subduction-related arc volcanic rocks and the E-MORB type basalts to the northwest of the studied area, our data evidenced the existence of a Early-Middle Permian arc-related basin in the Qinfang area.

ACKONWLEDGEMENTS

This work was supported by the Foundation of the Geological Survey of China [grant numbers 1212011220529 and 121201004000150021); a Key Research and Development Project of the Ministry of Science and Technology [grant number 2016YFC0601005] and NSFC [grant number 41372030]. We thank Prof. Wu Yuanbao for constructive comments and suggestions. We also thank the anonymous reviewers for their detailed and constructive reviews, which considerably improved the manuscript.

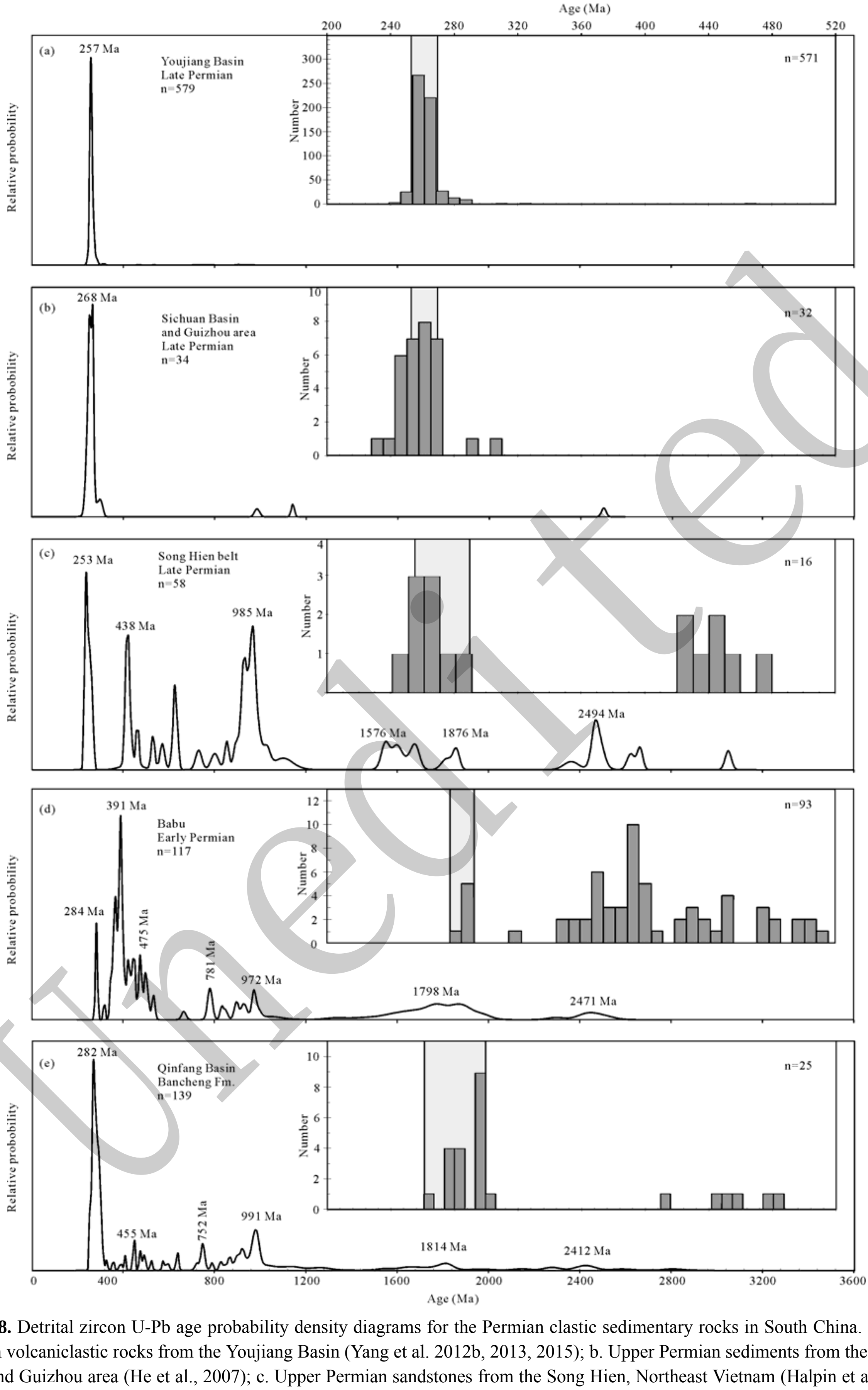

Figure 8. Detrital zircon U-Pb age probability density diagrams for the Permian clastic sedimentary rocks in South China. a. Upper Permian volcaniclastic rocks from the Youjiang Basin (Yang et al. 2012b, 2013, 2015); b. Upper Permian sediments from the Sichuan Basin and Guizhou area (He et al., 2007); c. Upper Permian sandstones from the Song Hien, Northeast Vietnam (Halpin et al. 2016); d. Upper Permian sandstones from Babu, Southeastern Yunnan; e. Bancheng Formation from the Qinfang Basin.

REFERENCES CITED

Belousova, E., Griffin,W., O'reilly, S.Y., et al., 2002. Igneous zircon: trace element composition as an indicator of source rock type. *Contrib. Mineral. Petrol*. 143: 602–622.

Bureau of Geology and Mineral Resources of Guangdong Province (BGMRGP). 1988. Regional Geology of Guangdong Province. Beijing: Geological Publishing House (in Chinese).

Bureau of Geology and Mineral Resources of Guangxi Zhuang Autonomous Region (BGMRGR), 1985. Geology of Guangxi Zhuang Autonomous Region. *Memoirs of the Geological Survey of China*, *1. Regional Geology, No. 3*. Beijing: Geological Publishing House (in Chinese).

Cai, J. X., Zhang, K. J., 2009. A new Model for the Indochina and South China Collision during the Late Permian to the Middel Triassic. *Tectonophysics*, 467 (1-4): 35-43.

Cawood, P. A., Hawkesworth, C., Dhuime, B., 2012. Detrital zircon record and tectonic setting. *Geology*, 40(10): 875–878.

Chen, C. H., Hsieh, P. S., Lee, C. Y., et al. Two episodes of the Indosinian thermal event on the South China Block: Constraints from LA-ICP-MS U-Pb zircon and electron microprobe monazite ages of the Darongshan S-type granitic suite. Gondwana Research. 2011. 19: 1008-1023.

Chen, C. H., Liu, Y. H., Lee, C. Y., et al. Geochronology of granulite, charnockite and gensis in the poly-metamorphosed Gaozhou Complex (Yunkai Massif), South China: Emphasis on the in-situ EMP monazite dating. Lithos, 2012, 106: 83-92.

Chen, Z., Lin, W., Faure, M., et al., 2014. Geochronology and isotope analysis of the Late Paleozoic to Mesozoic granitoids from northeastern Vienam and implications for the evolution fo the South China block. *Journal of Earth Sciences*, 86: 131-150.

Commission of China Stratigraphy, 2014. The Stratigraphic Chart of China. *Acta Geoscientica Sinica*, 35(3): illustration 1.

Condie, K.C., Belousova, E., Griffin, W.L., et al., 2009. Granitoid events in spaceand time: constraints from igneous and detrital zircon age spectra. *Gondwana Research*, 15:228–242.

Deng, X. G., Li, X. H., Chen, Z. G., 2003. Geochamical features and sedimentary setting of late Devonian chert in Bancheng of Qinzhou, Guangxi. *Chinese Journal of Geology*, 38(4): 460–469 (in Chinese with English abstract).

Deng, X.G., Chen, Z.Q., Li, X.H., et al., 2004. Shrimp U–Pb Zircon Dating of the Darongshan-Shiwandashan Granitoid belt in Southeastern Guangxi, China. Geological Review, 50(4): 426–432 (in Chinese with English abstract).

Fan, W. M., Wang, Y. J., Zhang, A. M., et al., 2010. Permian arc–back–arc basin development along the Ailaoshan tectonic zone: Geochemical，isotopic and geochronological evidence from the Mojiang volcanic rocks, Southwest China. *Lithos*, 119(3–4) : 553–568.

Halpin J. A., Tran H. T., Lai C. K., et al., 2016. U-Pb zircon geochronology and geochemistry from NE Vietnam: A 'tectonically disputed' territory between the Incochina and South China blocks. *Gondwana Research*, 34: 254-273.

He, B., Xu, Y. G., Huang, X. L., et al., 2007. Age and duration of the Emeishan flood volcanism, SW China: Geochemistry and SHRIMP zircon U-Pb dating of silicic ignimbrites, post-volcanic Xuanwei Formation and clay tuff at the Chaotian section. *Earth and Planetary Science Letters*, 255: 306-323.

He, W. H., Tang, T. T., Yue, M. L., et al., 2014. Sedimentary and Tectonic Evolution of Nanhua-Permian in South China. *Earth Science–Journal of China University of Geosciences*, 39(8): 929–953 (in Chinese with English abstract).

He, W. H., Zhang, Y., Zhang, Q., et al., 2011. A latest Permian radiolarian fauna from Hushan, South China, and its geological implications. *Alcheringa: An Australasian Journal of Palaeontology*, 35(4): 471-496.

Hennig D, Lehmann B, Frei D, et al. 2009. Early Permian seafloor to continental arc magmatism in the eastern Paleo-Tethys: U-Pb age and Nd-Sr isotope data from the southern Lancangjiang zone, Yunnan, China, Lithos, 113(3-4): 408-422.

Hoa, T. T.., Izokh, A. E., Polyakov, G. V., et al., 2008. Permo–Triassic magmatism and metallogeny of Northern Vietnam in relation to the Emeshan plume. *Russian Geology and Geophyisics*, 49: 480–491.

Hu, L. S., 2015. Permo-Triassic Tectonic Setting of the South China Block: Evidence from Contemporary Deposite Records. Doctoral Dissertation. Wuhan: China University of Geosciences (in Chinese with English abstract).

Hu, L. S., Cawood P A, Du Y S, et al., 2015. Detrital records for Upper Permian–Lower Triassic succession in the Shiwandashan Basin, South China and implication for Permo–Triassic (Indosinian) orogeny. *Journal of Asian Earth Sciences*, 98: 152–166.

Hu, L. S., Xu, Y. J., Du, Y. S., et al., 2014. Geochemical characteristics and its geological significance of the Late Paleozoic siliceous rocks in Qinfang Trough, southeastern Guangxi. *Journal of Palaeogeography*, 16 (1): 77–87 (in Chinese with English abstract).

Hu, Z.C., Gao, S., Liu, Y.S., et al., 2008. Signal enhancement in laser ablation ICP–MS by addition of nitrogen in the central channel gas. *Journal of Analytical Atomic Spectrometry*, 23: 1093–1101.

Hu, Z.C., Liu, Y.S., Gao, S., et al., 2012. A "wire" signal smoothing device for laser ablation inductively coupled plasma mass spectrometry analysis. *Spectrochimica Acta, Part B: Atomic Spectroscopy*, 78(0): 50–57.

Huang, G. C., Wang, X. W., Yang, S.Y., et al., 2001. Chronological evidence for the existence of the Meso-to Paleo-Proterozoic basement in the Yunkai uplift area. *Regional Geology of China* (in Chinese with English abstract).

Jian P, Liu D Y and Sun X M. 2008. SHRIMP dating of the Permo-Carboniferous Jinshajiang ophiolite, southwestern China: Geochronological constraints for the evolution of Paleo-Tehhys. Journal of Asian Earth Sciences, 32(5-6): 371-384.

Jian, P., Liu, D., Kröner, A., et al. 2009 a. Devonian to Permian plate tectonic cycle of the Paleo–Tethys Orogen in southwest China（Ⅰ): Geochemistry of Ophiolites, Arc/Back-Arc

Assemblages and Within-Plate Igneous Rocks, *Lithos*, 113(3–4): 748–766.
Jian, P., Liu, D., Kröner, A., et al., 2009 b. Devonian to Permian plate tectonic cycle of the Paleo–Tethys Orogen in southwest China (Ⅱ): Insights from zircon ages of ophiolites, arc/back–arc assemblages and within–plate igneous rocks and generation of the Emeishan CFB province. *Lithos*, 113(3–4): 767–784.
Jian, P., Wang, X. F., He, L. Q., et al., 1999. U-Pb zircon dating of anothosite and plagiogranite from the Jinshajiang ophiolite belt. *Acta Petrologica Sinica*, 15 (4): 590–593 (in Chinese with English abstract).
Kozur, H., 1993. Upper Permian radiolarians from the Sosio Valley Area, Western Sicily (Italy) and from the uppermost Lamar Limestone of West Texas. *Jahrbuch der Geologischen Bundesanstalt Wien*, 136, 99–123.
Lai, C. K., Meffre, S., Crawford, A. J., et al., 2014. The Central Ailaoshan ophiolite and modern analogs. *Gondwana Research*, 26:75–88.
Lepvrier, C., Maluski, H., Van, V, N., et al., 1997. Indosinian NW-trending shear zones within the Truong Son belt (Vietnam) ^{40}Ar-^{39}Ar Triassic ages and Cretaceous to Cenozoic overprints. *Tectonophysics*, 283: 105-127.
Li, Z. X., Li, X. H., 2007. Formation of the 1300-km-wide intracontinental orogen and postorogenic magmatic province in Mesozoic South China: A flat-slab subduction model. Geology, 35: 179-182.
Li, Z. X., Li, X. H., Zhou, H. W., et al., 2002. Grenvillian continental collision in south China: New SHRIMP U-Pb zircon results and implications for the configuration of Rodina. Geological Society of America, 30 (2): 163-166.
Li, X. H., Li, Z. X., He, B., et al., 2012. The Early Permian active continental margin and crustal growth of the Cathaysia Block: In situ U–Pb, Lu–Hf and O isotope analyses of detrital zircons. *Chemical geology*, 328: 195–207.
Li, X. H., Li, Z. X., Li, W. X., et al., 2006. Initiation of the Indosinian orogeny in South China: Evidence for a Permian magmatic arc on Hainan Island. *Jounal of Geology*, 114 (3): 341-353.
Li, Y. Y. 2013. Recognition and characteristics of the Lvchun island arc belt in the South of Jinsha River-Ailao Mountain Subduction-collision orgenic belt. Master's thesis. Chengdu: Chengdu University of Technology (in Chinese with English abstract).
Li, Z. X., Li, X. H., Li, W. X., et al., 2008. Was Cathaysia part of Proterozoic Laurentia?-new data from Hainan Island, south China. *Terra Nova*, 20:154-164.
Li, Z. X., Li, X. H., Wartho, J. A., et al., 2010. Magmatic and metamorphic events during the early Paleozoic Wuyi–Yunkai orogeny, southeastern South China: New age constraints and pressure–temperature conditions. *Geological Society of America Bulletin*, 122: 772–793.
Liang, X. Q. Li, X. H., 2005. Late Permian to Middle Triassic sedimentary records in Shiwandashan Basin: Implication for the Indosinian Yunkai Orogenic Belt, South China. *Sedimentary Geology*, 177(3-4): 297-320.
Liang, X. Q., Li, X. H., Qiu, Y. X., 2004. Intracontinental collisional orogeny during Late Permian-Middle Triassic in South China: Sedimentary records of the Shiwandashan Basin. *Acta Geologica Sinica*, 78(3): 756-762.
Liang, X. Q., Zhou, Y., Jiang, Y., et al., 2013. Study on LA-ICPMS U-Pb ages of detrital zircons from Upper Permian Wujiaping of Longtan Formation from the Yangtze and Cathaysia blocks. *Acta Petrologica Sinica,* 29(10): 3592-3606 (in Chinese with English abstract).
Liu, B., Feng, Q., Fang, N., et al. 1993b. Tectonic evolution of Palaeo-Tethys poly-island-ocean in Changning–Menglian and Lancangjiang Belts, Southwestern Yunnan, China. Journal of China University of Geosciences, 18, 529–539 (in Chinese with English abstract).
Liu, B. J., Xu, X. S., Pan, X. N., et al., 1993a. Paleocontinent Deposits, Crust revolution and Mineralization in Southern China. Beijing: China Science Publishing & Media Ltd. (in Chineses).
Liu, C., Deng, J. F., Liu, J. L., et al., 2011. Characteristics of volcanic rocks from Late Permian to Early Triassic in Ailaoshan tectono-magmatic belt and implications for tectonic setting. *Acta Petrologica Sinica*, 27(12): 3590-3602 (in Chinese with English abstract).
Liu, Y. S., Gao, S., Hu, Z. C., et al., 2010a. Continental and oceanic crust recycling–induced melt–peridotite interactions in the Trans–North China Orogen: U–Pb dating, Hf isotopes and trace elements in zircons of mantle xenoliths. *Journal of Petrology*, 51(1&2): 537–571.
Liu, Y. S., Hu, Z. C., Gao, S., et al., 2008. In situ analysis of major and trace elements of anhydrous minerals by LA–ICP–MS without applying an internal standard. *Chemical Geology*, 257(1–2): 34–43.
Liu, Y. S., Hu, Z. C., Zong, K. Q.,et al., 2010b. Reappraisement and refinement of zircon U–Pb isotope and trace element analyses by LA–ICP–MS. *Chinese Science Bulletin*, 55(15): 1535–1546.
Ludwig, K. R., 2003. ISOPLOT 3.00: A Geochronological Toolkit for Microsoft Excel. Berkeley Geochronology Center, California, Berkeley, 39 p.
Ma, W. P., 1996. Paleotethys in South China, Permian Orogeny and the Eastwards extension of Interchange Domain. *Scientia Geologica Sinica*, 31(2): 105-113 (in Chinese with English abstract).
Metcalfe, I. 2011. Paleozoic – Mesozoic history of SE Asia. In: Hall, R., Cottam, M.A. & Wilson, M.E.J. (eds) The SE Asian Gateway: History and Tectonics of the Australia–Asia Collision. Geological Society, London, Special Publications, 355, 7 – 35.
Peng, S. B., Jin, Z. M., Liu, Y. S., et al. 2006. Petrochemistry, chronology and tectonic setting of strong peraluminous anatectic granitoids in Yunkai Orogenic Belt, weatern Guangdong Province, China. Earth Science-*Journal of Earth Science*, 31(1):110-120 (in Chinese with English abstract).
Peng, S. B., Zhan, M. G., Zhang, Y. M., et al., 2000. Sm-Nd and Pb/Pb Isotopic Dating of Pre-Caledonian Granitic Rocks in Yunkai Area and its Significance. *ACTA Geoscientia Sinica-Bulletin of the Chinese Academy of Geological Sciences*, 21(1): 52-57 (in Chinese with English abstract).
Peng, T. P., Wang, Y. J., Zhao, G. C., et al. Arc-like volcanic rocks from the southern Lancangjiang zone, SW China:

Geochronological and geochemical constraints on their petrogenesis and tectonic implications. Lithos, 2008, 102(102): 358-373.

Qin, X. F., Pan, Y. M., Li, R. S., et al., 2006. Zircon SHRIMP U-Pb geochronology of the Yunkai metamorphic complex in southeastern Guangxi, China. *Geological Bulletin of China*, 25(5): 553-559 (in Chinese with English abstract).

Qin, X. F., Wang, Z. Q., Cao, J., 2013. Petrogenesis of Early Indosinian Granites from the Southwestern Segment of Qinfang Tectonic Belt, Southern Guangxi: Constraints from Zircon U-Pb Chronology and Geochemisty. *Journal of Jilin University (Earth Science Edition)*, 43(5): 1471-1487 (in Chinese with English abstract).

Qin, X. F., Wang, Z. Q., Zhang, Y. L., 2012. Geochemistry of Permian Mafic Igneous Rocks from the Napo-Qinzhou Tectonic Belt in Southwest Guangxi, SW China: Implications of Arc-Back Arc Basin Magmatic Evolution. *Acta Geologica Sinica*, 86(5): 1182-1199.

Qin, X. F., Wang, Z. Q., Zhang, Y. L., et al., 2011. Geochronology and Geochemistry fo Early Mesozoic Acid Volcanic Rocks from Southwest Guangxi: Constraints on Tectonic Evolution of the Southwestern Segment of Qinzhou-Hangzhou Joint Belt. *Acta Petrologica Sinica*, 27(3): 794-808(in Chinese with English abstract).

Roger, F., Leloup, P. H., Jolivet, M., et al., 2000. Long and complex thermal history of the Song Chay metamorphic dome (northern Vietnam) by multi–system geochronology. *Tectonophysics*, 321:449–466.

Roger, F., Maluski, H., Lepvrier, C., et al., 2012. LA-ICPMS zircons U/Pb dating of Permo-Triassic and Cretaceous magmatisms in Northern Vietnam-Geodynamical implications. *Journal of Asian Earth Sciences*, 48: 72-82.

Sone, M. and Metcalfe, I., 2008. Parallel Tethyan sutures in mainland Southeast Asia: New insight for Palaeo–Tethys closure and implications for the Indosinian orogeny. *C.R.Geoscience*, 340(2–3): 166–179.

Sone, M., Metcalfe, I., Chaodumrong, P., 2012. The Chanthaburi terrane of southeastern Thailand: Stratigraphic confirmation as a disrupted segment of the Sukhothai Arc. *Journal of Asian Earth Sciences*, 61: 16–32.

Sun, D. Y., Xia, W. C., 2006. Identification of the Guadalupian–Lopingian boundary in the Permian in a bedded chert sequence, South China. *Paleogeography, Palaeoclimatology, Palaeoecology*, 236: 272–289.

Tang, L. M., Chen, H. L., Dong, C. W., et al., 2013. Middle Triassic post-orogenic extension on Hainan Island: Chronology and geochemistry constraints of bimodal intrusive rocks. Science China: Earth Sciences, 56 (5): 783-793.

Wang, X., Metcalfe, I., Jian, P., et al. 2000. The Jinshanjiang–Ailaoshan Suture Zone, China: Tectostratigraphy, age and evolution. Journal of Asian Earth Sciences, 18, 675–690.

Wang ,Y. J., Fan, W. M., Zhang, G. W., et al. 2013. Phanerozoic tectonics of the South China Block: key observations and controversies. *Gondwana Research* , 23(4): 1273-1305.

Wang, Y. S.，Liu, D. Y.，Xu, M. H., et al. 2007. SHRIMP U-Pb zircon geochronology and geochemistry of metavolcanic and metasedimentary rocks in Northwestern Fujian, Cathaysia block, China: Tectonic implications and the need to redefine lithostratigraphic units. *Gondwana Research*, 12 : 166-183.

Wang, Y. J., 1994. Chert and its Radiolarian Assemblage of the Qinzhou Area, Guangxi. *Chinese Science Bulletin*, 39 (13): 1208–1210 (in Chinese).

Wang, Y. J., Luo, D., Kuang, G. D., et al., 1998. Late Devonian–Late Permian Strata of Cherty Facies at Xiaodong and Bancheng Counties of the Qinzhou Area, SE Guangxi. *Acta Micropalaeontologica Sinica*, 15 (4): 351–366 (in Chinese with English abstract).

Wang, Y. J., Luo, H. and Yang, Q., 2012. Late Paleozoic Radiolarians in the Qinfang area, southeast Guangxi: Anhui, University of Science and Technology of China, 127 p., 22 pls (in Chinese).

Wang, Y. J., Wu, C. M., Zhang, A. M., et al., 2011. Kwangsian and Indosinian reworking of the eastern South China Block: Constraints on zircon U–Pb geochronology and metamorphism of amphibolites and granulites. *Lithos*, 127:239–260.

Wiedenbeck, M., Alle, P., Corfu, F., et al., 1995. Three natural zircon standards for U-Th-Pb, Lu-Hf, trace element and REE analyses. Geostandards and Geoanalytical Research, 19(1): 1-23.

Wu, G. Y., Ji, J. Q., He, S. D., et al. 2002. Early Permian Magmatic Arc in Pingxiang, Guangxi and its Tectonic Implications. *Journal of Mineralogy and Petrology*, 22 (3): 61-65.

Wu, G. Y., Zhong, D. L., Zhang, Q., et al., 1999. Babu-Phy Ngu Ophiolites: A Geological Record of Paleotethyan Ocean Bordering China and Vietnam. *Gondwana Research*, 2(4): 554-557.

Wu, H. R., 1999. Implications of Rdiolarian Chert for the Palaeogeography of South China. *Journal of Palaeogeography*, 1 (2): 28–35 (in Chinese with English abstract).

Wu, H. R., 2003. Discussion on Tectonic Palaeogeography of Nanpanjiang Sea in the Late Palaeozoic and Triassic. *Journal of Palaeogeography*, 5 (1): 63–76 (in Chinese with English abstract).

Wu, H. R., Xian, X. Y., Kuang, G. D. 1994 b. Late Paleozoic Radiolarian Assemblages of Southern Guangxi and its Geological Significance. *Scientia Geologica Sinica*, 29(4): 339–345 (in Chinese with English abstract).

Wu, H. R., Xian, X. Y., Kuang, G. D., et al., 1994 a. Late Paleozoic Radiolarian Chert of South Guangxi and the preliminary discussion on the Tethys of Guangxi. *Chinese Science Bulletin*, 39(9): 809–812 (in Chinese).

Xie, C. F., Zhu, J. C., Ding, S. J., et al., 2006. Identification of Hercynian shoshonitic intrusive rocks in central Hainan Island and its geotectonic implications. *Chinese Sciences Bulletin*, 51 (20): 2507-2519.

Xu, D. M., Lin, Z. Y., Long, W. G., et al., 2012. Research History and Current Situation fo Qinzhou-Hangzhou Metallogenic Belt, South China. *Geology and Mineral Resources of South China*, 28(4): 277-289.

Xu, X. S., Yin, F. G., Wan, F., et al., 2001. The migration of the Qinzhou-Fancheng trough in Guangxi and associated sedimentary-tectonic transform surfaces. *Sedimentary*

Geology and Tethyan Geology, 21(4): 1-10 (in Chinese with English abstract).

Yan D P, Zhou M F, Wang C Y, et al. 2006. Structural and geochronological constraints on the tectonic evolution of the Dulong–Song Chay tectonic dome in Yunnan Province, SW China. *Journal of Asian Earth Sciences*, 28: 332–353.

Yang J. H., Cawood P. A., Du Y. S., et al., 2015. Voluminous silicic eruptions during late Permian Emeishan igneous province and link to climate cooling. *Earth and Planetary Science Letters*, 432: 166-175.

Yang, J. H., Cawood, P. A., Du, Y. S. et al., 2014. A sedimentary archive of tectonic switching from Emeishan Plume to Indosinian orogenic sources in SW China. *Journal of the Geological Society*, 171: 269–280.

Yang, J. H., Cawood, P. A., Du, Y. S., et al., 2012 a. Detrital record of Indosinian mountain building in SW China: Provenance of the Middle Triassic turbidites in the Youjiang Basin. *Tectonophysics*, (574–575): 105–117.

Yang, J. H., Cawood, P. A., Du, Y. S., et al., 2012 b. Large Igneous Province and magmatic arc sourced Permian–Triassic volcanogenic sediments in China. *Sedimentary Geology*, 261–262: 120–131.

Yang, J. H., Cawood, P. A., Du, Y. S., et al., 2013. A Sedimentary Archive of Tectonic Swithing from Emeishan Plume to Indosinian Orogenic Sources in SW China. *Journal of the Geological Society, London*, 171 (2): 269-280.

Yang, J. H., Du, Y. S., Yu, X., et al., 2017. Early Permian Volcanic Fragments-Bearing Sandstones in Babu of Southeastern Yunnan Indicative of Paleo-Tethyan Ocean Subduction. *Earth Science*, 42(1): 24-34 (in Chinese with English abastract).

Yang, M. G., Mei, Y. W., 1997. Characteristics of Geology and Metatllization in the Qinzhou-Hangzhou Paleoplate Juncture. *Geology and Mineral Resources of South Chin*a, 9(3): 52-59 (in Chinese with English abstract).

Yang, W. Q., Feng, Q. L., Liu, G. C., 2010. Radiolarian Fauna and Geochemical Characters of the Cherts from Garz-Litang Tectonic Belt and Its Tectono-Paleogeographic Significance. Acta Geologica Sinica, 84(1): 78-88.

Yu, J. H., O'Reilly, S. Y., Wang, L., et al., 2010. Components and episodic growth of Precambrian crust in the Cathaysia Block, South China: evidence from U-Pb ages and Hf isotopes of zircons in Neoproterozoic sediments. *Precambrian Research*, 181: 97-114.

Yu, Z. Z., Shi, Y. S., Guo, L. Z., 1989. The Paleocontourite and its Tectonic Significance in Qinzhou Basin, Guangxi, China. *Acta Sedimentologica Sinica*, 7(3): 21–29 (in Chinese with English abstract).

Zhang, A. M., Wang, Y. J., Fan, W. M., et al., 2012. Earliest Neoproterozoic (ca. 1.0 Ga) arc-back-arc-basin nature along the northern Yunkai Domain of the Cathaysia Block: geochronological and geochemical evidence from the metabasite. *Precambrian Research*, 220-221: 217-233.

Zhang, B. H., Ding, J., Zhang, L. K., et al., 2013. SHRIMP Zircon U-Pb Chronology of the Babu Ophiolite in Southeastern Yunnan Province. ACTA Geologica Sinica, 87 (10): 1498-1509 (in Chinese with English abstract).

Zhang, K. X., He, W. H., Luo, M. S., et al., 2016. Sedimentary Formations and Sedimentary Tectonic Revolution of China. Beijing: Geological Publishing House (in Chinese with English abstract).

Zhang, N., Xia, W. C., 1998. Time-Space Distribution of Late Paleozoic Cherts and Evolution of Respreading Trench in South China. *Earth Science–Journal of China University of Geosciences*, 23 (5): 124–131 (in Chinese with English abstract).

Zhang, N., Xia, W. C., Dong, Y. X., et al., 2008. Conodonts and radiolarians from pelageic cherts of the Frasnian–Famennian boundary interval at Bancheng, Guangxi, China: Global recognition of the upper Kellwasser event. *Marine Micropaleontology*, 67: 180–190.

Zhang, N., Xia, W. C., Shao, J., 2002. Radiolarian successional sequences and rare earth element variations in Late Paleozoic chert sequences of South China: an integrated approach for study of the evolution of paleo–ocean basin. *Geomicrobiology Journal*, 19: 439–460.

Zhao, L., Guo, F., Fan, W.M., et al., 2010. Crustal evolution of the Shiwandashan area in South China: Zircon U–Pb–Hf isotopic records from granulite enclaves in Indo-Sinian granites. Chinese Science Bulletin, 55: 2028–2038.

Zhao, X. K., Yong, Z. Q., Li, G. R., 2007. Residual basin of passive continental margin—a neglected basin type. *Oli & Gas Geology*, 28(1): 121-128 (in Chinese with English abstract).

Zhong, D. L., Wu, G. Y., Ji, J. Q., et al., 1998. Discovery of the Ophiolite in Southeast Yunnan. *Chinese Science Bulletin,* 43(13): 1365–1370 (in Chinese).

Zhou Y, Bohor B F, Ren, Y. 2000. Trace element geochemistry of altered volcanic ash layers (tonsteins) in Late Permian coal-bearing formations of eastern Yunnan and western Guizhou Provinces, China. International Journal of Coal Geology, 44, 305 – 324.